

TIT/HEP-329/NP
May,1996

Nuclear G-Matrix Elements from Nonlocal Potentials

K. Yoshida, A. Hosaka^(a), and M. Oka

Department of Physics, Tokyo Institute of Technology
Meguro, Tokyo 152, Japan

^(a)Numazu College of Technology
3600 Ooka, Numazu 410, Japan

e-mail: kyoshida@th.phys.titech.ac.jp
hosaka@la.numazu-ct.ac.jp
oka@th.phys.titech.ac.jp

Abstract

We study effects of nonlocality in the nuclear force on the G-matrix elements for finite nuclei. Nuclear G-matrix elements for ^{16}O are calculated in the harmonic oscillator basis from a nonlocal potential which models quark exchange effects between two nucleons. We employ a simple form of potential that gives the same phase shifts as a realistic local nucleon potential. The G-matrix elements calculated from the nonlocal potential show moderate increase in repulsion from those derived from the local potential.

1 Introduction

Several models of the nucleon-nucleon interaction have been presented and applied to nuclear physics problems. The G-matrix interaction plays a central role in calculations of nuclear structure from the nucleon-nucleon (NN) interaction, as it is the basic two-body interaction in many body systems.

It is well known that the nucleon-nucleon interaction is described by the quark cluster model (QCM). This model gives a good description of the nucleon-nucleon scattering [1, 2]. The main feature of the interaction is nonlocality at short distances. This short range potential has a nonlocal Gaussian soft core of the form,

$$V(\mathbf{r}', \mathbf{r}) \propto \exp[-(\frac{\mathbf{r} - \mathbf{r}'}{b})^2].$$

This type of nonlocality is expected from the quark antisymmetrization between the baryons. The Gaussian form reflects the quark wave function inside the baryon and the nonlocality range parameter b is determined by the size of the baryon. The nonlocal exchange force can reproduce the short-range repulsion of the nuclear force at low energy. The repulsive “core” in QCM is a soft core with energy dependence in its equivalent local form. It allows the NN relative wave function to go inside and thus gives a milder form factor of the deuteron (or nuclei) at large momenta [3]. Because the quark exchange nonlocality comes only at short distances, the central part of the potential is most affected. In fact, the NN repulsion is roughly spin-isospin independent.

In this paper, we would like to study significance of the nonlocality of quark model origin in nuclear structure calculations. Since we can not see signals of such nonlocality in on-shell properties, it would be interesting if we could see them in nuclear phenomena. To do so, we calculate G-matrix elements from nonlocal potentials. In conventional nuclear physics, the G-matrix interaction is used as the basic two-body interaction for the nuclear many-body problem. Hence, if there would be signals of quark-originated nonlocality in nuclear phenomena, they must exist in the G-matrix interaction as well. Previously, effects of symmetry restoration of QCD in G-matrix elements were examined [4]. Thus in the present study we investigate another possibility of QCD oriented effects in nuclear physics.

This paper is organized as follows. In section 2, a method to calculate G-matrix elements for finite nuclei is given briefly. In section 3, we introduce the Tamagaki G3RS (Gaussian soft core potential with three ranges) potential [5] as a local potential. Then we construct a nonlocal Gaussian soft core potentials, which has the same intermediate and long range parts as the original local potential. The short-range part is replaced by a nonlocal potential with free parameters which are determined so as to reproduce the same scattering phase shifts as the local potential. In section 4, numerical results for the G-matrix elements are given both for the local and nonlocal potentials. A summary is given in section 5.

2 Nuclear G-matrix for Finite Nuclei

The G-matrix is the most fundamental two body interaction which incorporates the simplest many body effect, i.e., the Pauli blocking. It is obtained by solving the Bethe-Goldstone

equation [6]:

$$G(E) = v + v \frac{Q}{E - H_0} G(E). \quad (1)$$

Here v is a nucleon-nucleon interaction in free space, Q the Pauli-blocking operator, and H_0 a single particle hamiltonian. We compute G-matrix elements for finite nuclei, specifically for ^{16}O , following the method developed in previous works [7, 8, 9]. H_0 is chosen to be the harmonic oscillator hamiltonian. The two-body problem is then reduced to a one-body problem of the relative coordinate by employing the Eden and Emery's approximation [10] for the Q operator. Explicitly, after reducing the Pauli-blocking operator as a function of the relative coordinate, it is assumed to be

$$Q(n') = \begin{cases} 1 & \text{for } n' > n + 2 \\ 0 & \text{otherwise} \end{cases} \quad (2)$$

where n is the node quantum number for the relative motion of the initial two nucleons and n' that for intermediate states. The Barret-Hewitt-MacCarthy's method [11] is then used for matrix inversion. Additional parameter is introduced for the gap energy, which is chosen to be 40 MeV to achieve a good agreement between the calculated G-matrix elements and empirical ones [12]. Finally, the starting energy is averaged over the Fermi surface by assuming that the relevant two nucleons are there.

G-matrix elements are obtained first in partial wave channels denoted by 1S_0 , 1P_1 , etc., which are then transformed into those in interaction channels denoted by SE (Singlet Even), TE (Triplet Even), etc. Matrix elements in SE and SO (Singlet Odd) channels are just those in 1S_0 and 1P_1 channels, respectively. The TE and TNE (Tensor Even) components are obtained from the coupled $^3S_1 - ^3D_1$ channels:

$$G(\text{TE}) = \langle S | G(^3S_1 - ^3D_1) | S \rangle, \quad (3)$$

$$G(\text{TNE}) = \langle S | G(^3S_1 - ^3D_1) | D \rangle. \quad (4)$$

The TO, TNO, LSO (LS Odd) and LSE (LS Even) components are obtained from the following relations [7]:

$$G(\text{TO}) = G(^3P_0) + 2G(\text{LSO}) + 4G(\text{TNO}), \quad (5)$$

$$G(\text{TNO}) = -\frac{5}{72}[2G(^3P_0) - 3G(^3P_1) + G(^3P_2)], \quad (6)$$

$$G(\text{LSO}) = -\frac{1}{12}[2G(^3P_0) + 3G(^3P_1) - 5G(^3P_2)], \quad (7)$$

$$G(\text{LSE}) = -\frac{1}{60}[9G(^3D_1) + 5G(^3D_2) - 14G(^3D_3)], \quad (8)$$

In the previous studies [7, 8, 9], the Reid soft-core potential, Paris potential, and other phenomenological nuclear forces have been applied. We here choose the Tamagaki G3RS potential [5], which is a three range gaussian with a short range soft core. We replace the shortest-range part of the original potential by a nonlocal one, and apply it to the G-matrix calculation. The resulting G-matrix elements are compared with each other.

3 Gaussian Nonlocal Potential

We use the following Tamagaki potential as a standard local potential,

$$V_L(\mathbf{r}) = V_C(r) + S_{12}V_T(r) + (\mathbf{L} \cdot \mathbf{S})V_{LS}(r) + W_{12}V_W(r) + \mathbf{L}^2V_{LL}(r), \quad (9)$$

with

$$\begin{aligned} S_{12} &= 3(\sigma_1 \cdot \mathbf{r})(\sigma_2 \cdot \mathbf{r})/r^2 - \sigma_1 \cdot \sigma_2 \\ W_{12} &= 1/2\{(\sigma_1 \cdot \mathbf{L})(\sigma_2 \cdot \mathbf{L}) + (\sigma_2 \cdot \mathbf{L})(\sigma_1 \cdot \mathbf{L})\} - (\sigma_1 \cdot \sigma_2)\mathbf{L}^2/3 \\ &= (\mathbf{L} \cdot \mathbf{S})^2 - \{\delta_{LJ} + (\sigma_1 \cdot \sigma_2)/3\}\mathbf{L}^2 \end{aligned}$$

where L and J stand for the orbital and total angular momenta, respectively. The radial functions $V_n(r)$ ($n = C, LS, \dots$) are given by

$$V_n(r) = \sum_{i=1}^3 V_{ni} \exp[-(r/\eta_{ni})^2], \quad (10)$$

where the suffices $i = 1, 2, 3$ refer to the short range, intermediate range and long range part, respectively. The potential parameters, V_{ni} and η_{ni} , are determined so as to reproduce the scattering phase shifts as given in Table 1 [5].

The nonlocal potential is constructed by replacing the short range part ($i = 1$) of Eq. (10). We consider nonlocality only for the central part of the form:

$$V(\mathbf{r}', \mathbf{r}) = V_{NL}(\pi^{1/2}b)^{-3} \exp[-(\frac{\mathbf{r} - \mathbf{r}'}{b})^2 - (\frac{\mathbf{r} + \mathbf{r}'}{\eta_{NL}})^2] \quad (11)$$

Similar nonlocal terms might appear in noncentral forces, but for the reason explained in introduction, we consider the nonlocality only in the central potential. In Eq. (11), the factor $(\pi^{1/2}b)^{-3} \exp[-(\frac{\mathbf{r} - \mathbf{r}'}{b})^2]$ represents the nonlocality of the nuclear force at short distances, with a new parameter b as the range of nonlocality. When $b \rightarrow 0$, this part reduces to the delta function, $\delta(\mathbf{r} - \mathbf{r}')$, and then the nonlocal potential becomes the local one. In the quark cluster model, b is proportional to the size of the quark wave function in the nucleon. A typical value of b would be 0.5 fm, which we use in the following calculations.

In order to study effects of nonlocality exclusively, we require the nonlocal potential to reproduce the same scattering phase shifts as the corresponding local potential does. We call such a nonlocal potential as local-equivalent (LE) nonlocal potential. For this, we adjust the potential parameters, V_{NL} and η_{NL} . We allow them to depend on the angular momentum L . Phase shifts in various partial waves at scattering energies from $E_{cm} = 0$ to 300 MeV are fitted. As shown in Figs. 1 - 2, both the local and LE nonlocal potentials (LENL) reproduce empirical phase shifts well up to the scattering energy ~ 300 MeV. In particular, the difference between the local and LENL are negligibly small. In Figs. 1 and 2, we also present the phase shifts calculated from the nonlocal potentials (NL) with the same strength, $V_{NL} = V_{C1}$ and the same range $\eta_{NL} = \eta_{C1}$ as the original Tamagaki potential. They show that the nonlocality yields a softer repulsion at large energy. Although we have shown here the phase shifts only for the two channels, we find qualitatively the same feature for other S and P channels.

	η_{C_1} V_{C_1}	η_{C_2} V_{C_2}	η_{C_3} V_{C_3}	η_{T_1} V_{T_1}	η_{T_2} V_{T_2}	η_{T_3} V_{T_3}	η_{LS_2} V_{LS_2}	η_{LS_3} V_{LS_3}	η_{W_2} V_{W_2}	η_{LL_2} V_{LL_2}
<i>SE</i>	0.447 2000	0.942 -270	2.5 -5							0.942 15
<i>TO</i>	0.447 2500	0.942 -70	2.5 1.67	0.447 -20	1.2 20	2.5 2.5	0.447 600	0.6 -1050	0.942 0	0.942 0
<i>SO</i>	0.447 2000	0.942 50	2.5 10							0.942 0
<i>TE</i>	0.447 2000	0.942 -230	2.5 -5	0.447 67.5	1.2 -67.5	2.5 -7.5	0.447 0	0.6 0	0.942 -30	0.942 30

Table 1: Parameters of the Tamagaki G3RS potential

	$\eta_{NL}^{b=0.5}$	$V_{NL}^{b=0.5}$
$l = 0$	$0.894 \times \eta_{C_1}$	$1.45 \times V_{C_1}$
1	$0.894 \times \eta_{C_1}$	$2.9 \times V_{C_1}$
2	$0.894 \times \eta_{C_1}$	$6.0 \times V_{C_1}$
3	$0.894 \times \eta_{C_1}$	$12.5 \times V_{C_1}$
4	$0.894 \times \eta_{C_1}$	$27 \times V_{C_1}$

Table 2: Parameters of the nonlocal potential with $b = 0.5$ fm

Summarizing, our LE nonlocal potential reads

$$\begin{aligned}
V_{NL}(\mathbf{r}', \mathbf{r}) = & V_{NL}(\pi^{1/2}b)^{-3} \exp[-(\frac{\mathbf{r} - \mathbf{r}'}{b})^2 - (\frac{\mathbf{r} + \mathbf{r}'}{2\eta_{NL}})^2] \\
& + \sum_{i=2}^3 V_{C_i} \exp[-(r/\eta_{C_i})^2] \delta(\mathbf{r} - \mathbf{r}')
\end{aligned} \tag{12}$$

with the parameters given in Table 1 for the local part and in Table 2 for the nonlocal part ($b = 0.5$ fm).

4 Numerical Results

The G-matrix elements in the harmonic-oscillator basis are presented in Tables 3–4 for the local (Tamagaki) and LE nonlocal potentials with $b = 0.5$ fm as functions of node quantum numbers n and n' . These are calculated using an oscillator parameter $\hbar\omega = 14$ MeV for ^{16}O and with the gap energy of 40 MeV, which are the same as those used in Refs. [7, 8, 9].

First we compare G-matrix elements calculated from various nuclear forces. For this purpose, we show in Table 5 the G-matrix elements derived from the Paris potential and those of the present calculation for the SE channel. It turns out that both matrix elements are very similar. The difference is significant only for less important off-diagonal matrix elements, which

	s s	n=0	n=1	n=2	n=3
singlet	n'=0	-6.605	-5.182	-3.551	-2.064
even	1		-4.564	-3.251	-1.831
	2			-2.352	-1.233
	3				-0.428
	s s	n=0	n=1	n=2	n=3
triplet	n'=0	-10.495	-8.725	-6.488	-4.401
even	1		-7.982	-6.209	-4.274
	2			-5.028	-3.525
	3				-2.468
	p p	n=0	n=1	n=2	n=3
singlet	n'=0	2.365	2.140	1.768	1.495
odd	1		2.614	2.575	2.374
	2			2.905	2.935
	3				3.202
	p p	n=0	n=1	n=2	n=3
triplet	n'=0	0.200	0.057	-0.052	-0.098
odd	1		0.039	-0.005	-0.031
	2			0.030	0.059
	3				0.144
	s d	n=0	n=1	n=2	n=3
tensor	n'=0	-5.391	-7.403	-8.463	-9.011
even	1	-2.429	-4.688	-6.463	-7.691
	2	-0.967	-2.449	-4.067	-5.502
	3	-0.338	-1.095	-2.208	-3.454
	p p	n=0	n=1	n=2	n=3
tensor	n'=0	0.772	0.745	0.639	0.535
odd	1		0.896	0.872	0.782
	2			0.940	0.908
	3				0.939
	d d	n=0	n=1	n=2	n=3
LS	n'=0	-0.034	-0.048	-0.057	-0.062
even	1		-0.075	-0.091	-0.102
	2			-0.117	-0.133
	3				-0.156
	p p	n=0	n=1	n=2	n=3
LS	n'=0	-0.416	-0.666	-0.850	-0.983
odd	1		-0.998	-1.247	-1.432
	2			-1.536	-1.753
	3				-1.990

Table 3: G-matrix elements from the local potential for ^{16}O

	s s	n=0	n=1	n=2	n=3
singlet	n'=0	-6.542	-5.098	-3.444	-1.931
even	1		-4.460	-3.126	-1.683
	2			-2.213	-1.076
	3				-0.260
	s s	n=0	n=1	n=2	n=3
triplet	n'=0	-10.499	-8.714	-6.457	-4.343
even	1		-7.962	-6.171	-4.212
	2			-4.978	-3.458
	3				-2.392
	p p	n=0	n=1	n=2	n=3
singlet	n'=0	2.372	2.150	1.780	1.507
odd	1		2.627	2.591	2.392
	2			2.924	2.955
	3				3.224
	p p	n=0	n=1	n=2	n=3
triplet	n'=0	0.206	0.064	-0.046	-0.093
odd	1		0.046	0.000	-0.028
	2			0.032	0.056
	3				0.134
	s d	n=0	n=1	n=2	n=3
tensor	n'=0	-5.400	-7.421	-8.491	-9.048
even	1	-2.439	-4.707	-6.493	-7.732
	2	-0.978	-2.469	-4.097	-5.543
	3	-0.348	-1.114	-2.236	-3.493
	p p	n=0	n=1	n=2	n=3
tensor	n'=0	0.772	0.745	0.639	0.537
odd	1		0.897	0.873	0.784
	2			0.942	0.912
	3				0.944
	d d	n=0	n=1	n=2	n=3
LS	n'=0	-0.034	-0.048	-0.057	-0.062
even	1		-0.075	-0.091	-0.102
	2			-0.117	-0.134
	3				-0.157
	p p	n=0	n=1	n=2	n=3
LS	n'=0	-0.414	-0.663	-0.849	-0.983
odd	1		-0.997	-1.248	-1.436
	2			-1.541	-1.762
	3				-2.006

Table 4: G-matrix elements from LE nonlocal potential ($b=0.5\text{fm}$) for ^{16}O

	n'	$n = 0$	$n = 1$	$n = 2$	$n = 3$
Tamagaki	0	-6.605	-5.182	-3.551	-2.064
	1		-4.564	-3.251	-1.831
	2			-2.352	-1.233
	3				-0.428
Paris	0	-6.580	-5.292	-3.743	-2.502
	1		-4.644	-3.322	-1.947
	2			-2.386	-1.070
	3				-0.318

Table 5: Comparison of diagonal G-matrix elements in the SE channel derived from three nuclear forces.

is, however, typically 20 % level. This is interesting because the Tamagaki potential has the Gaussian tail and its functional form differs from the others. This fact suggests that G-matrix elements are strongly constrained by on-shell properties (phase shifts). We have confirmed this by calculating G-matrix elements using NN potentials which do not necessarily reproduce empirical phase shifts.

Now we turn to see the effects of nonlocality in the G-matrix elements. From Tables 3-4, one sees that for non-central channels of tensor and LS, the results of the local and of LE nonlocal potentials are almost identical. This seems natural because in the present calculation nonlocality is introduced only in the central channel.

Effects of nonlocality in the G-matrix elements are best seen in the S-wave channels of SE and TE. They are repulsive, though the effects are typically as small as a few % or even less. Therefore, one may conclude that the present nonlocality from the quark exchange effects are negligibly small as compared with other many-body effects of nuclear physics which is typically about 10 % or even more [12]. The reason that the present nonlocality acts as repulsive is understood in the following way. As we have discussed in section 3, when nonlocality is introduced for a repulsive component, it effectively reduces the repulsion in the NN potential. To get the local-equivalent phase shifts, one has to modify the potential parameters by reducing the range and increasing the strength of repulsion as summarized in Table 2. In the calculation of the G-matrix elements, the Pauli-blocking operator Q forbids the transition to lower levels which are already occupied. This effectively reduces the chance for the two nucleons to feel attraction in the nuclear force which comes mainly from the transition to the lower states. Hence, in the G-matrix elements, repulsive components are more enhanced.

The nonlocal effect would become important for heavier nuclei where more levels are Pauli blocked. We have performed a calculation of G-matrix elements in the zirconium region. The calculation was done in the same way as for ^{16}O , but with $\hbar\omega = 8.8$ MeV and with the following Pauli-blocking operator:

$$Q(n') = \begin{cases} 1 & \text{for } n' > n + 4, \\ 0 & \text{otherwise.} \end{cases} \quad (13)$$

Here, as the mass number is increased, more states are Pauli-blocked, which is implemented in the inequality $n' > n + 4$ in place of $n' > n + 2$ for ^{16}O in (2). Results are summarized in Table

	n'	$n = 0$	$n = 1$	$n = 2$	$n = 3$
local	0	-3.922	-3.551	-2.926	-2.291
	1		-3.449	-2.961	-2.360
	2			-2.612	-2.114
	3				-1.718
LE nonlocal	0	-3.812	-3.422	-2.787	-2.145
	1		-3.299	-2.800	-2.191
	2			-2.440	-1.934
	3				-1.533

Table 6: G-matrix elements in the SE channel for zirconium

6 for the SE channel, where we see slightly more nonlocal effects. The difference is, however, once again very small.

5 Summary

The G-matrix elements for ^{16}O have been calculated in the harmonic oscillator basis from a G3RS Tamagaki potential (local potential) and a nonlocal potential which has a simple Gaussian nonlocality at a short range but produces the same scattering phase shifts as the local potential does. The nonlocal Gaussian soft core is typical of quark cluster model (QCM) which gives a good description of the nucleon-nucleon scattering.

The G-matrix elements thus derived from the nonlocal potential show an effective repulsion in comparison with those derived from the local potential. The difference appears in the SE and TE channels mostly. The effects are, however, generally very small for all nuclei. It is not, therefore, likely that quark-originated nonlocal effects are detected in conventional nuclear phenomena.

References

- [1] M. Oka and K. Yazaki, *Phy. Lett.* **B90** (1980) 41; *Prog. Theor. Phys.* **66** (1981) 556; **66** (1981) 572; *in Quarks and Nuclei*, ed. by W. Weise (World Scientific, 1985); K. Shimizu, *Rep. Prog. Phys.* **52** (1989) 1; S. Takeuchi, K. Shimizu and K. Yazaki, *Nucl. Phys.* **A504** (1989) 777
- [2] M. Oka, *in Proceedings of 10th International Symposium on High Energy Spin Physics*, Nagoya, Nov, 1992
- [3] M. Oka and K. Yazaki, *Nucl. Phys.* **A402** (1983) 477; S. Takeuchi, K. Shimizu and M. Oka, *Nucl. Phys.* **481** (1988) 693
- [4] A. Hosaka and H. Toki, *Nucl. Phys.* **A529** (1991) 429
- [5] R. Tamagaki, *Prog. Theor. Phys.* **39** (1968) 91

- [6] H. A. Bethe, *Ann. Rev. Nucl. Part. Sci.* **21** (1971) 93
- [7] G. F. Bertsch et al, *Nucl. Phys.* **A284** (1977) 399
- [8] N. Anantaraman, H. Toki and G. F. Bertsch, *Nucl. Phys.* **A398** (1983) 269
- [9] A. Hosaka, K. -I. Kubo and H. Toki, *Nucl. Phys.* **A444** (1985) 76
- [10] R. J. Eden and V. J. Emery, *Proc. Roy. Soc. London.* **A248** (1958) 226
- [11] B. R. Barrett, R. G. L. Hewitt and R. J. McCarthy, *Phys. Rev.* **C3** (1971) 1137
- [12] B.A. Brown, W.A. Richter, R.E. Julies and B.H. Wildenthal, *Ann. of Phys.* **182** (1988) 191.

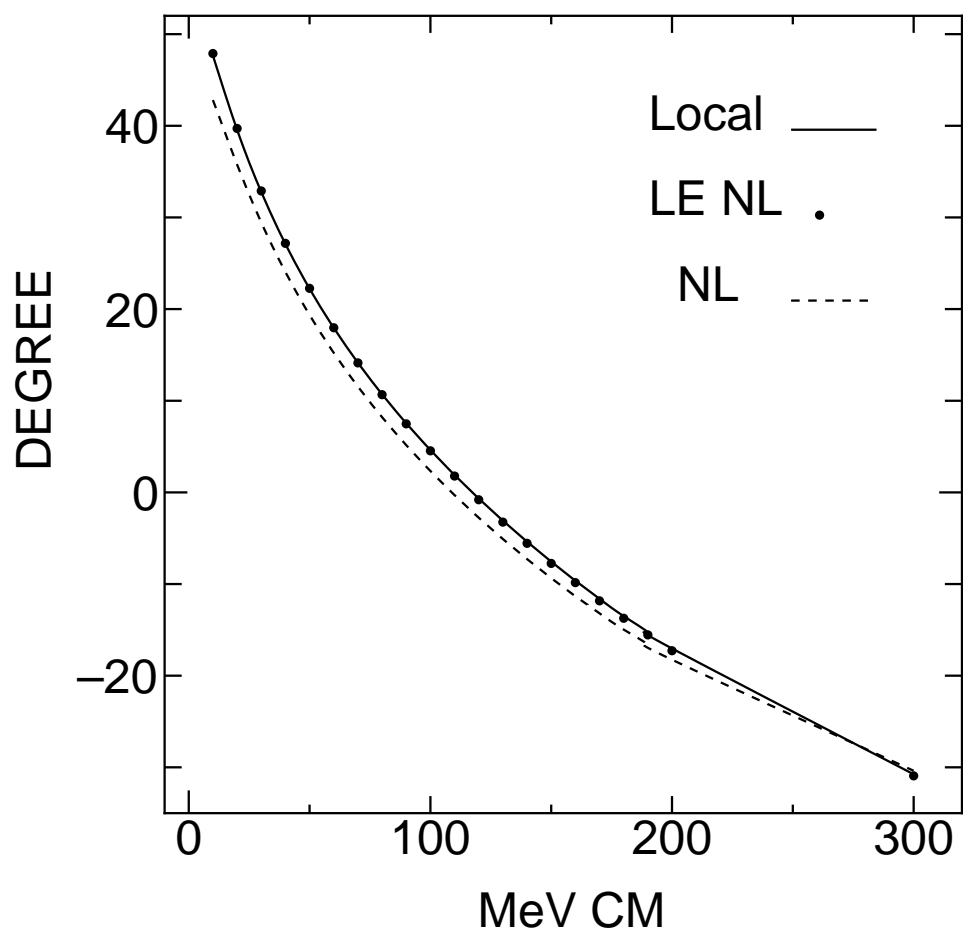


Figure 1: NN scattering phase shifts in the 1S_0 channel for the local, LENL and NL potentials.

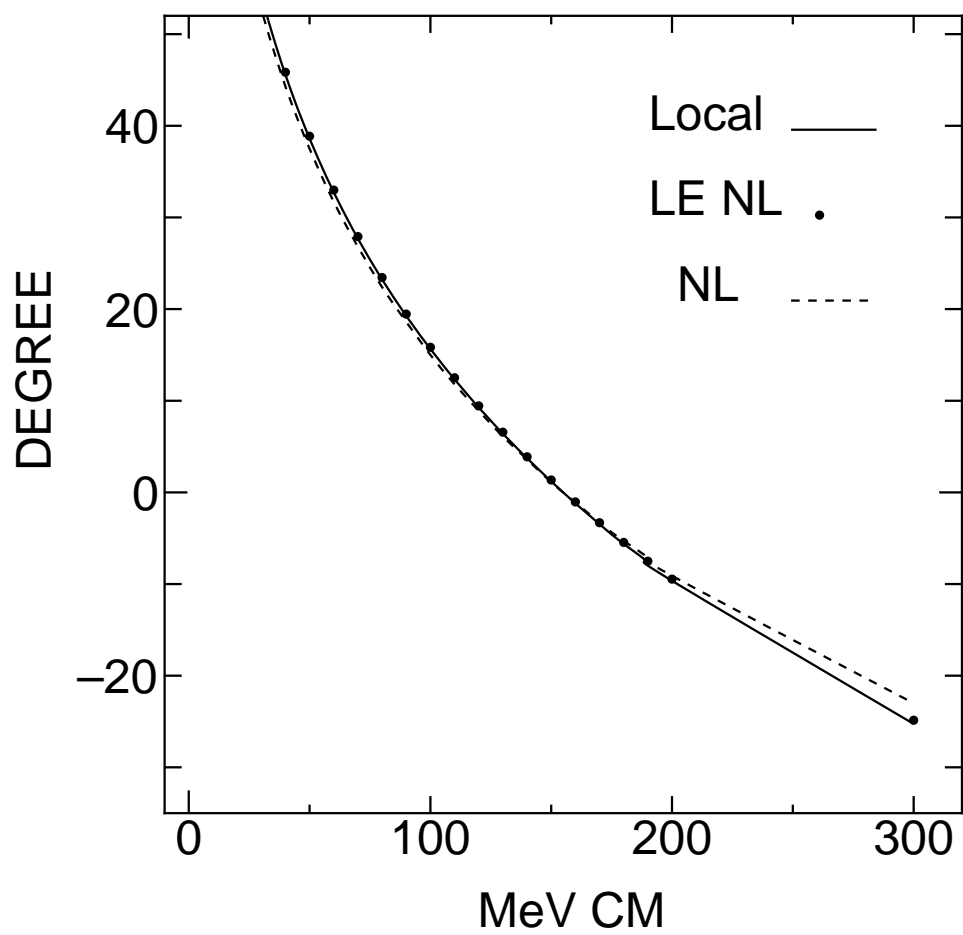


Figure 2: NN scattering phase shifts for 3S_1 .